

Using phase transitions to investigate the effect of salts on protein interactions

Michael L. Broide,* Tina M. Tominc, and Marc D. Saxowsky
Department of Physics, Lewis and Clark College, Portland, Oregon 97219

(Received 16 October 1995)

We have investigated liquid-liquid and solid-liquid phase separation of aqueous solutions of lysozyme. We have determined experimentally how the phase transition temperatures depend on protein concentration and the ionic composition of the solution. For a wide range of solution conditions, we find that the cloud-point temperature T_{cloud} —which signals the onset of liquid-liquid phase separation—is 15–45 °C below the crystallization temperature T_{xtal} . This indicates that liquid-liquid phase separation occurs in a highly metastable solution. When a series of chloride, bromide, and sulfate salts are added to lysozyme, we find that T_{cloud} varies by as much as 60 °C over the salt concentration range of 0.2M to 1.5M. The precise change in T_{cloud} depends sensitively on the identities of both the cation and the anion of the added salt. The effect of salts on T_{xtal} is very similar to their effect on T_{cloud} . The Derjaguin-Landau-Verwey-Overbeek theory for the interaction energy between charged spheres cannot account for our observations and indicates that hydration forces play an important role in protein interactions. [S1063-651X(96)09106-4]

PACS number(s): 87.15.-v, 64.70.Ja, 64.75.+g, 82.70.Dd

INTRODUCTION

The interaction between protein molecules underlies many biological, chemical, and technological processes. These interactions play a crucial role in the behavior of highly concentrated protein solutions. The interior of a biological cell, for example, is an extraordinarily crowded environment [1–3]: red blood cells contain about 35% protein by weight, muscle cells contain 23% protein, eye lens cells [4] contain up to 60% protein.

An effective way to determine the strength of protein interactions is to study temperature-induced phase transitions that occur in concentrated protein solutions. In this paper, we investigate liquid-liquid and solid-liquid phase separation of aqueous lysozyme solutions. We determine experimentally how the phase boundaries depend on protein concentration and the ionic composition of the solution. Changes in the phase boundaries reveal subtle changes in the interaction energy between proteins because these interactions are what drive the phase transitions. Our data can be used to test and refine theoretical models [5,6] for the interaction energy between macromolecules.

The phenomenon of liquid-liquid phase separation, also known as coacervation [7], occurs when a protein solution is cooled below its cloud-point temperature T_{cloud} . The solution then separates into two coexisting liquid phases: one rich in protein and one poor in protein. The onset of liquid-liquid phase separation is associated with a dramatic clouding of the solution due to the formation of domains of protein-rich and protein-poor phases. Liquid-liquid phase separation has been studied extensively in liquid mixtures [8], in polymer solutions [9], and in micellar solutions [10]. Much less work has been reported for protein solutions.

In 1977, Ishimoto and Tanaka [11,12] measured the liquid-liquid phase boundary for lysozyme. Taratuta *et al.* [13] subsequently measured the effects of salts and pH on

the cloud-point temperature of lysozyme. Our experiments build upon the work of Taratuta *et al.* We have extended the range and types of salts previously studied, and we have measured both the liquid-liquid and solid-liquid phase boundaries of lysozyme. The well-documented physical and chemical properties of lysozyme [14–16] make it a convenient model system.

The crystallization or solid-liquid phase separation of protein solutions has been widely investigated [17–21]. The solubility of a protein depends on many physical and chemical factors, including the nature of the protein, solution pH, concentration of salts, and concentration of organic compounds. A number of empirical techniques have been developed to grow protein crystals, but a complete theoretical understanding of the art of protein crystallization is still evolving.

The nucleation and growth of protein crystals can take weeks or months [22–24]. This slow time scale makes it difficult to undertake systematic investigations of the effect of solution conditions on protein solubility. In contrast, the onset of liquid-liquid phase separation takes seconds or minutes [25], enabling one to quickly examine the effects of solution conditions on protein interactions. Our experiments show that the phase boundaries for liquid-liquid and solid-liquid phase separation are strongly correlated. This suggests that liquid-liquid phase separation can be used to efficiently identify the optimum solution conditions for growing protein crystals. Furthermore, it may be easier to develop a theoretical model for the interactions that govern liquid-liquid phase separation than it is to develop one for the intricate process of solid-liquid separation.

Protein interactions play a role in several diseases, such as cataracts [26,27], sickle cell anemia [28], and cryoimmunoglobulinemia [29]. Benedek and co-workers [30–35] have investigated the phase behavior of calf lens proteins in connection with the formation of cold cataracts. San Biagio and Palma [36] have determined the spinodal lines in solutions of normal and sickle-cell human hemoglobin. These studies indicate that a deeper understanding of protein interactions

*Electronic address: broide@lclark.edu

may suggest strategies for treating or preventing certain diseases.

MATERIALS AND METHODS

Sample preparation

Hen eggs white lysozyme is a globular protein with a molecular mass of 14 400 daltons containing 129 amino acid residues [37]. Its shape is roughly ellipsoidal, with dimensions $45 \times 30 \times 30 \text{ \AA}^3$. At pH 7.8, lysozyme has a net charge of +8 electronic charges; its isoelectric pH is 11.2 [15].

Lysozyme was obtained from Sigma Chemical (L7001, crystallized three times) and used without additional purification. The powdered protein was dissolved in the buffer selected for a particular experiment, which was generally 20 mM HEPES (*N*-[2-Hydroxyethyl]piperazine-*N'*[2-ethanesulfonic acid]), pH 7.8. After stirring at room temperature, the solution was filtered through a 0.22- μm syringe filter to remove any undissolved protein. The concentration of lysozyme at this stage was typically 25 mg/ml. An Amicon ultrafiltration device equipped with a YM-10 membrane was used to concentrate the protein solution and to wash away low-molecular-weight impurities. The final lysozyme concentration was 200–250 mg/ml. This concentrated solution did not grow protein crystals due to the low ionic strength of the buffer.

To conduct our experiments it is essential that we have a routine method for preparing protein solutions that are free of crystals. In past work by Taratuta *et al.* [13], the protein solution was dialyzed against the salt solutions of experimental interest. This procedure can take several days and by the time the dialysis is completed, the protein solution often crystallizes. To overcome this problem, we prepared the protein solution at roughly twice the final desired concentration and added to it a doubly concentrated salt solution. The benefit of this approach is that the salt ions are introduced into the protein solution moments before the sample is analyzed. Measurements can be performed before the salt induces the formation of protein crystals. The speed and convenience of this method of sample preparation enabled us to explore a wide range of salt concentrations and identities.

The salts and buffers used were reagent grade. Salt solutions were prepared gravimetrically, and in the case of hydrated salts, CaCl_2 and MgCl_2 , the concentrations were confirmed by EDTA (ethylenediamine tetra-acetic acid) titration [38]. Solution pH was adjusted by adding small amounts of concentrated NaOH or HCl as needed. We were careful not to exceed the solubility of any of the salts in our experiments. All solutions contained 3 mM sodium azide to inhibit bacterial growth.

Once the stock solutions for the protein and salt were made, the experimental samples were mixed as needed. Precisely measured volumes of the protein and salt solutions were pipetted into an 8 mm \times 30 mm test tube and vortexed. The total sample volume was usually 150 μl . Approximately 12 μl of the sample was drawn into a microcapillary for the crystallization experiments. The test tube was then sealed and placed in a thermostated water bath to determine the cloud-point temperature of the sample.

The pH of each experimental sample was checked using pH indicator strips with a resolution of 0.2 pH units. There

was a slight variation, ± 0.4 pH units, but control experiments described in the Results section demonstrate that this level of uncertainty in pH is acceptable for our study.

Lysozyme concentrations were determined using UV absorption spectroscopy. A small aliquot (typically 5–10 μl) of the protein sample under investigation was diluted with buffer solution, and the UV absorption of the resulting solution was measured. The specific absorbance coefficient for lysozyme used in this study is $E_{280}^{0.1\%,1\text{ cm}} = 2.64$ [16].

To check that our procedure for sample preparation was repeatable, each batch of protein was “calibrated.” A portion of each batch was mixed with NaCl from 0.20 to 1.5 M and the cloud-point temperatures were determined; for an example of such a curve see Fig. 3. The cloud-point temperatures for each batch agreed to within 0.5 $^\circ\text{C}$.

Determination of phase boundaries

Following Taratuta *et al.* [13], samples were placed in a thermostated water bath equipped with a laser beam transmission apparatus to monitor the turbidity of the sample. The onset of liquid-liquid phase separation is associated with a dramatic clouding of the solution due to the formation of domains of protein-rich and protein-poor phases. The temperature of the bath, which has a precision of 0.1 $^\circ\text{C}$, was lowered in steps until the transmission fell to 70% of its initial value, T_{70} . The sample was then heated by raising the temperature in small steps until it became clear again. The clarification temperature is denoted T_{clear} , and it was typically 1 to 3 $^\circ\text{C}$ above T_{70} , depending on the protein concentration. The observed hysteresis has been noted before [13,31] and it is presumably due to the fact that the sample must be undercooled to induce the phase transition. The phase boundary lies between T_{70} and T_{clear} , and we use the average of these two temperatures to estimate the liquid-liquid boundary. We refer to this average temperature as simply “the cloud-point temperature,” T_{cloud} . Cloud-point measurements were performed immediately after a sample was prepared and before protein crystals had a chance to form.

Solid-liquid phase boundaries were determined using an optical microscope equipped with a temperature-controlled stage (Physitemp TS-4ER), following the technique of Berland *et al.* [32]. Rectangular microcapillaries (Vitro Dynamics) with dimensions $50 \times 2 \times 0.2 \text{ mm}^3$ were used to hold the samples. Capillaries were plugged with Critoseal vinyl plastic putty and the ends were sealed with Superglue (cyanoacrylate ester) to prevent evaporation. They were then set aside at room temperature, or in some cases at 3 $^\circ\text{C}$, until lysozyme crystals with a linear dimension of about 100 μm grew. The thermostated stage allowed us to heat and cool samples with a precision of 0.1 $^\circ\text{C}$. The temperature was raised in small steps until the crystals began to dissolve. Next, we cooled the sample to regrow the facets of the crystals and then heated the sample in finer temperature steps until we determined the dissolving temperature—which we refer to as T_{xtal} —to within 0.5 $^\circ\text{C}$. A video recording of the process helped us to detect accurately the minimum temperature at which the sharp edges of a crystal rounded.

In the course of our investigation we observed two distinct crystal habits (Fig. 1): prisms and needles. For identical solution conditions, we find that the dissolving temperature

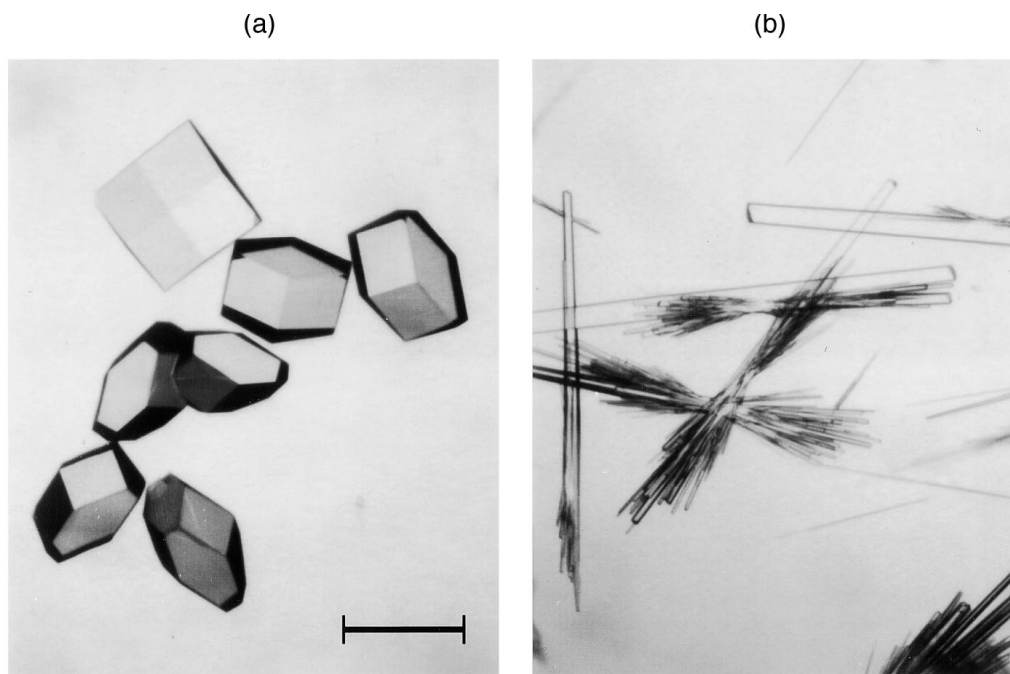


FIG. 1. Examples of the two lysozyme crystal habits we observed: (a) prisms, (b) needles. Scale bar is $200\ \mu\text{m}$. Often both habits grow under identical solution conditions; we find that the dissolving temperature of needles is $5\text{--}10\ ^\circ\text{C}$ higher than the dissolving temperature of prisms. All solid-liquid boundaries in subsequent figures are for prisms.

for needles is $5\text{--}10\ ^\circ\text{C}$ greater than the dissolving temperature for prisms. Previous work has been shown that lysozyme solubility depends on crystal form [39–43]. Presumably the different intermolecular contacts associated with each crystal form result in different crystal binding energies. From the crystal habit alone, we cannot deduce the crystal form, but the figures in Durbin and Feher [44] suggest that the prisms we observe are tetragonal lysozyme crystals. All of the solid-liquid boundaries reported in this paper are for prisms.

The dissolving temperature of a crystal depends on the concentration of protein solution that is in contact with it (Fig. 2). Stated differently, a protein's solubility depends on temperature. Therefore, it is important that the protein concentration in the capillary is uniform. This required that we measure the dissolving temperature when only a few minute crystals were present. To verify that the concentration was not significantly reduced by the crystals, we would rapidly cool the sample to determine the cloud-point temperature, which is a sensitive measure of protein concentration (Fig. 2). If the clouding was spatially uniform and at the predicted temperature, we concluded that protein concentration gradients in the capillary were negligible.

The solid-liquid phase boundary can also be determined by measuring the solubility of protein at a fixed temperature [32]. However, we found, as others have [22,23], that it can take weeks or months for the system to equilibrate. The dynamic technique we use enables us to determine the dissolving temperature in a few hours once minute crystals form.

For completeness, we determined the solubility of lysozyme at room temperature. After a cloud-point measurement was taken, the test tube containing the protein was set aside at room temperature, $23 \pm 2\ ^\circ\text{C}$, and crystals were allowed to grow. Every few weeks we determined the concen-

tration of protein in the supernatant. Our procedure was to vortex the sample, centrifuge it, and then remove an aliquot of supernatant for UV analysis. Data were collected until the concentration of the supernatant stopped decreasing, which typically took several weeks to months depending on the sample.

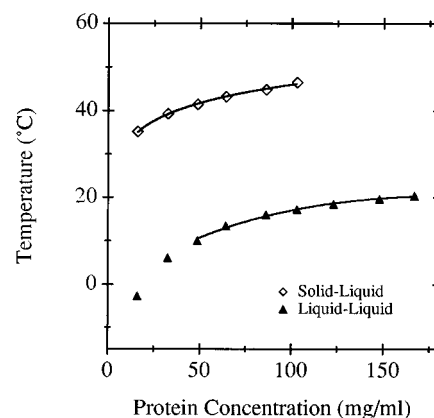


FIG. 2. Phase diagram for aqueous lysozyme solution (20 mM HEPES buffer, $\text{pH}\ 7.8$, 0.5M NaCl). The upper curve is the solid-liquid phase boundary; the lower curve is the liquid-liquid phase boundary. The liquid-liquid boundary is $30\text{--}40\ ^\circ\text{C}$ below the solid-liquid phase boundary. The solid lines represent Eqs. (1) and (2). For temperatures and protein concentrations below the solid-liquid boundary, the equilibrium state of the system consists of a mixture of protein crystals coexisting with a saturated protein solution. When a supersaturated protein solution is cooled rapidly it undergoes liquid-liquid phase separation prior to crystallizing. (In Figs. 2–7 the size of the symbols used to plot the data is comparable or larger than the uncertainty in the data.)

RESULTS

Effect of protein concentration on phase transitions

In Fig. 2 we plot the solid-liquid (T_{xtal}) and liquid-liquid (T_{cloud}) phase boundaries for lysozyme for a range of protein concentration (C). The solution conditions are 20 mM HEPES buffer pH 7.8M, and 0.5M NaCl. This figure demonstrates that the liquid-liquid phase boundary lies 30–40 °C below the solid-liquid phase boundary, which implies that liquid-liquid phase separation takes place in a highly metastable solution. We are able to determine both phase boundaries because the time scale for crystal formation is much slower than the time scale for the formation of a protein-rich liquid phase. This metastable behavior was previously observed in four different calf lens protein solutions [32], indicating that it may be a general feature of concentrated protein solutions.

Following Broide *et al.* [31], we fit the liquid-liquid phase boundary in Fig. 2 to the function

$$|(C_c - C)/C_c| = A[(T_c - T)/T_c]^\beta, \quad (1)$$

where $\beta = 0.325$, C_c is the critical protein concentration, T_c is the critical temperature in K, and A is a parameter that characterizes the width of the coexistence curve. Setting $C_c = 230$ mg/ml based on the results of Taratuta *et al.* [13], we find that $T_c = 20.6 \pm 0.5$ °C and $A = 2.4 \pm 0.2$. (Only the data within 10 °C of T_c were used in the fit.) It is interesting to note that for the calf lens proteins, $A = 2.6 \pm 0.1$, suggesting that the width of the liquid-liquid phase boundary does not depend critically on the identity of the protein.

Following Ewing, Forsythe, and Pusey [40], we fit the solid-liquid phase boundary using van't Hoff's equation:

$$\ln C = \Delta H/RT + B, \quad (2)$$

where ΔH is the change in enthalpy for the formation of a protein crystal, B is a fitting parameter associated with the change in entropy, and R is the molar gas constant. Note that C is in mg/ml and T is in Kelvin. Fitting Eq. (2) to the solid-liquid boundary in Fig. 2, we find that $\Delta H = -138 \pm 5$ kJ/mol and $B = 57 \pm 2$. As expected, the change in enthalpy is negative, indicating that heat is released when a crystal forms. Solubility experiments on lysozyme report much smaller magnitudes for the enthalpy. Ewing, Forsythe, and Pusey [40] find that $\Delta H = -32$ kJ/mol for orthorhombic lysozyme crystals in 0.5M NaCl, pH 4.0. Cacioppo and Pusey [39] find that $\Delta H = -87$ kJ/mol for tetragonal lysozyme crystals in 0.3M NaCl, pH 4.0. Differences in solution condition and crystal forms may account for the disparate enthalpy values. Alternatively, the trouble may lie in using Eq. (2) to fit the data, as Cacioppo and Pusey [39] point out.

Berland *et al.* [32] have developed a rigorous thermodynamic model to interpret the solid-liquid phase boundary. This theory enables one to deduce the free-energy change ε associated with transferring one protein molecule and the corresponding stoichiometric number of water molecules from the solution phase into the solid phase. We find that ε has a characteristic value of about $8kT_c$, where k is Boltzmann's constant, and $T_c = 293.8$ K as deduced from Eq. (1) above. The free energy ε decreases roughly linearly with

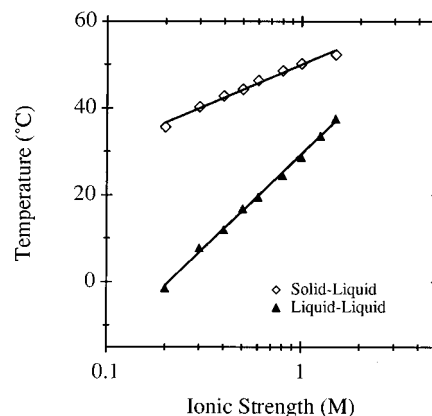


FIG. 3. Dependence of T_{cloud} and T_{xtal} on added NaCl (20 mM HEPES, pH 7.8; lysozyme concentration 87 mg/ml). The solid lines are empirical fits to the data, Eqs. (3), indicating that T_{cloud} and T_{xtal} increase approximately linearly with the log of NaCl concentration.

increasing temperature according to the formula $\varepsilon(T) = 42.8 - 0.110T$, where T is in Kelvin. The magnitude and temperature dependence of ε for lysozyme are very similar to what Berland *et al.* found for the calf lens proteins. [We used the following values for the parameters in Eq. (9) for $\varepsilon(T)$ in Berland *et al.* [32]: $\gamma = 562$, $\kappa = 429$ for tetragonal lysozyme crystals [42], and $\theta_D = 100$ K.]

Effect of salts on phase transitions

Changing the salt concentration of the solution shifts the phase boundaries in Fig. 2 up or down in temperature, but the basic shape of the curves can still be accounted for by Eqs. (1) and (2) with suitable parameters.

Figure 3 shows how the phase boundaries change as the concentration of NaCl is varied from 0.20M to 1.5M. The buffer is 20 mM HEPES pH 7.8; the protein concentration is fixed at 87 mg/ml. Over the entire range of salt concentration studied, the liquid-liquid phase boundary is below the solid-liquid boundary. We further note that the two boundaries are strongly correlated: when T_{cloud} increases, so does T_{xtal} . This correlation is further discussed in Figs. 4 and 5.

The linearity of the semilogarithmic plot in Fig. 3 implies that T_{cloud} and T_{xtal} increase approximately linearly with the log of the NaCl concentration. The solid lines in Fig. 3 are an empirical fit to the data:

$$T_{\text{cloud}} = 29.28 + (43.11)\log_{10}[\text{NaCl}], \quad (3a)$$

$$T_{\text{xtal}} = 49.98 + (19.12)\log_{10}[\text{NaCl}], \quad (3b)$$

where the salt concentration is in moles/l (M) and temperature is in °C. Extrapolating the two boundaries in Fig. 3 suggests that they cross at high salt concentration. Setting $T_{\text{cloud}} = T_{\text{xtal}} = T^*$ in Eq. (3) we find that $T^* = 66.5$ °C, which

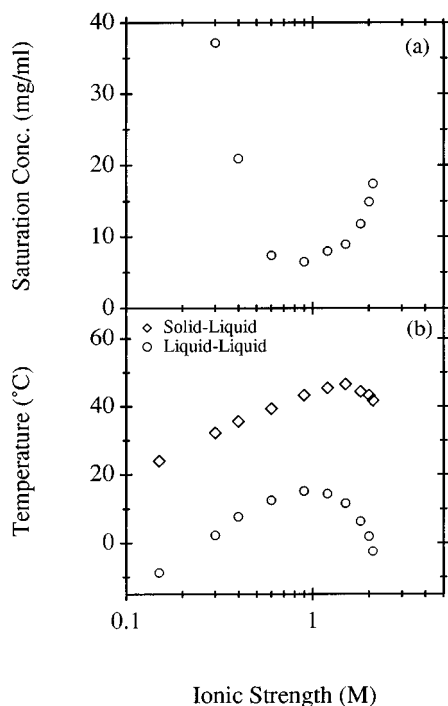


FIG. 4. Effect of MgBr_2 on phase boundaries (20 mM HEPES, pH 7.8). (a) Solubility of lysozyme at $T = 23 \pm 2^\circ\text{C}$ as a function of added MgBr_2 . (b) Dependence of T_{cloud} and T_{xtal} on added MgBr_2 (lysozyme concentration 87 mg/ml). Note the strong correlation between T_{cloud} , T_{xtal} , and protein solubility.

occurs when $[\text{NaCl}] = 7.3\text{M}$. This salt concentration is above the saturation concentration of NaCl, making it experimentally inaccessible. It is intriguing that lysozyme appears to denature at approximately T^* , based on the fact that for temperatures above 65°C the protein precipitates irreversibly.

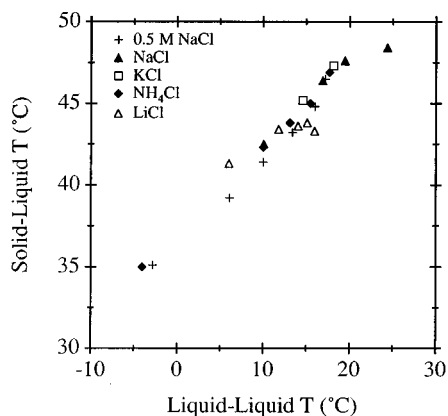


FIG. 5. For a variety of solution conditions, T_{xtal} and T_{cloud} are uniquely correlated. The (+) data are taken from Fig. 2 and correspond to fixed NaCl concentration, variable protein concentration. The (\blacktriangle) data are taken from Fig. 3 and correspond to fixed protein concentration, variable NaCl concentration. For the other salts, the protein concentration is fixed (87 mg/ml) and the salt concentration is varied.

In Fig. 3, and in much of what follows, the protein concentration is fixed at 87 ± 5 mg/ml. To appreciate how concentrated this is, at 87 mg/ml the average distance between the surfaces of two lysozyme molecules is 32 \AA [14], about the diameter of the protein. We chose this value for the concentration to facilitate comparison of our results with those of Taratuta *et al.* [13], who used a protein concentration of 90 mg/ml. Furthermore, this high protein concentration enables us to obtain more precise data for T_{cloud} and T_{xtal} . According to Fig. 2, at a protein concentration of 87 mg/ml, an uncertainty of 5 mg/ml in the concentration results in an uncertainty of 0.5°C in T_{cloud} and 0.4°C in T_{xtal} . At a lower protein concentration, the slopes of the curves in Fig. 2 are greater, and a small uncertainty in protein concentration would result in a larger uncertainty in the phase transition temperatures.

Figure 4(b) demonstrates how the phase boundaries vary with the addition of MgBr_2 . As before, the buffer is 20 mM HEPES, pH 7.8, and the protein concentration is 87 mg/ml. The concentration range of MgBr_2 is from 0.05M to 0.70M, corresponding to a range of ionic strength from 0.15M to 2.10M. We find, in similarity to Fig. 3 for NaCl, that the liquid-liquid boundary is below the solid-liquid boundary, and that the two boundaries are strongly correlated. In contrast to Fig. 3, the boundaries in Fig. 4(b) do not grow monotonically with increasing salt concentration. Instead, they exhibit a peak at an ionic strength of about 1M and then decrease.

In Fig. 4(a), we plot the solubility of lysozyme at room temperature, $23 \pm 2^\circ\text{C}$, as a function of the ionic strength of MgBr_2 . We see that the solubility is minimum at about 1M. Thus, the room-temperature solubility of lysozyme reaches a minimum when the cloud-point temperature is at a maximum. The data at Fig. 4 demonstrate that T_{cloud} provides an alternate (and rapid) means of determining the effect of salt on protein solubility: When T_{cloud} is low, the solubility of the protein is high; when T_{cloud} is high, the solubility of the protein is low.

The correlation between T_{xtal} and T_{cloud} is further demonstrated in Fig. 5. Here we have replotted the data from Fig. 2 (fixed NaCl concentration, variable protein concentration) and Fig. 3 (variable NaCl concentration, fixed protein concentration). Figure 5 also contains data for three other monovalent salts, where the protein concentration is fixed (87 mg/ml) and the salt concentration is varied. The alignment of the data points in Fig. 5 is striking and indicates that the correlation between T_{xtal} and T_{cloud} holds for a variety of solution conditions. This shows that the forces that govern these two phase transitions are affected similarly by changes in the solution conditions.

Having established the importance of the liquid-liquid phase boundary, we present in Fig. 6 the effect of a variety of monovalent and divalent salts on the cloud-point temperature of lysozyme. Once again, the buffer is 20 mM HEPES, pH 7.8, and the protein concentration is 87 mg/ml. For clarity, we divide the data into three groups: chloride salts [Fig. 6(a)], bromide salts [Fig. 6(b)], and sulfate salts [Fig. 6(c)]. The cloud-point data from Figs. 3 and 4(b) are included in Fig. 6 to facilitate comparison.

The data in Fig. 6 demonstrate that both the identity of the salt and its ionic strength affect T_{cloud} , in accord with

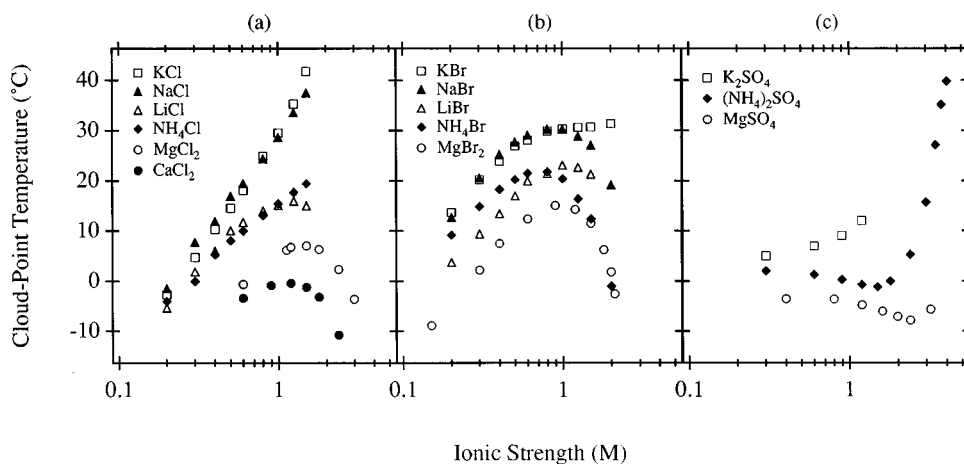


FIG. 6. Effect of salt concentration and type on the cloud-point temperature (20 mM HEPES, pH 7.8; lysozyme concentration 87 mg/ml). The cloud-point temperature is highly dependent on the identity of the added salt. This reveals that the underlying protein interactions are also affected by ion identity. There are many intriguing anion and cation trends in the data.

Taratuta *et al.* [13]. From a theoretical perspective, this implies that the magnitude of the Debye screening length alone does not determine T_{cloud} . The interaction energy between protein molecules is critically dependent on the identity of the salt ions in solution. We now describe our experimental observations in detail:

Chloride data [Fig. 6(a)]: The effects of NaCl and KCl on T_{cloud} are very similar, and for both salts T_{cloud} increases essentially linearly with the log of salt concentration over the range of 0.20 to 1.5M. The data for NaCl are fully discussed in connection with Fig. 3. The data for LiCl and NH_4Cl lie on a common curve, which is below the line for NaCl and KCl. The divalent salts, MgCl_2 and CaCl_2 , show dramatically different behavior from the monovalent salts. Above ionic strengths of 1M, T_{cloud} decreases with increasing salt concentration for MgCl_2 and CaCl_2 . The simple behavior exhibited in the NaCl and KCl data is clearly not typical.

Bromide data [Fig. 6(b)]: The effects of NaBr and KBr on T_{cloud} are very similar, and below 1M salt concentration T_{cloud} for these salts is above T_{cloud} for NaCl and KCl. For salt concentrations above 1M, T_{cloud} levels off for KBr, and it decreases for NaBr. T_{cloud} for LiBr is below the curves for NaBr and KBr. As discussed in Fig. 4(b), T_{cloud} exhibits a peak at about 1M for MgBr_2 , much like the data for MgCl_2 and CaCl_2 . For NH_4Br , T_{cloud} decreases above 1M, much like the data for the divalent salts and in contrast to the data for NH_4Cl .

Sulfate data [Fig. 6(c)]: The sulfate data are markedly different from the chloride and the bromide data. The effect of $(\text{NH}_4)_2\text{SO}_4$ is especially intriguing. For ionic strengths from 0.2M to 1.0M, T_{cloud} decreases slightly with increasing $(\text{NH}_4)_2\text{SO}_4$ concentration. For the chloride and bromide salts, T_{cloud} always increased over this range of ionic strength. Above 1M $(\text{NH}_4)_2\text{SO}_4$, T_{cloud} increases dramatically with increasing ionic strength. We note that $(\text{NH}_4)_2\text{SO}_4$ is frequently used to precipitate or crystallize proteins [45]. The low solubility of K_2SO_4 and MgSO_4 limited the range of ionic strength we could explore with these salts.

For ionic strengths below 1M, we can make some generalization based on Fig. 6. For a given anion, T_{cloud} decreases in the following order:

$$\begin{aligned} (\text{high } T_{\text{cloud}}) \text{K}^+ \approx \text{Na}^+ > \text{Li}^+ \approx \text{NH}_4^+ > \text{Mg}^{2+} \\ > \text{Ca}^{2+} (\text{low } T_{\text{cloud}}). \end{aligned} \quad (4)$$

For example, for two salt solutions of identical ionic strength, T_{cloud} for NaCl is greater than T_{cloud} for LiCl; T_{cloud} for K_2SO_4 is greater than T_{cloud} for MgSO_4 , and so forth. In fact, with the exception of the data for NaBr and NH_4Br the above cation ranking holds for ionic strengths above and below 1M.

In Fig. 7, we replot a portion of the cloud-point data from Fig. 6 to examine the role that anions play in protein interactions. Note the similar ordering of the curves in Figs. 7(a), 7(b), and 7(c). We first consider the bromide and chloride data. For ionic strengths below 1M, the cloud-point temperature decreases in the following order:

$$(\text{high } T_{\text{cloud}}) \text{Br}^- > \text{Cl}^- (\text{low } T_{\text{cloud}}). \quad (5a)$$

Between 1M and 2M, depending on the salt, the bromide and chloride curves cross, and thus for high ionic strengths T_{cloud} decreases in the following order:

$$(\text{high } T_{\text{cloud}}) \text{Cl}^- > \text{Br}^- (\text{low } T_{\text{cloud}}). \quad (5b)$$

This implies that one cannot rank the effect of these anions on T_{cloud} without also specifying if the ionic strength is below or above the crossing point of the cloud-point curves.

It is hard to draw conclusions about the sulfate salts due to the limited range of the data. At low ionic strengths, T_{cloud} for the sulfate salts is generally below T_{cloud} for the chloride salts. At high ionic strengths, above 2M–3M, T_{cloud} for $(\text{NH}_4)_2\text{SO}_4$ is greater than T_{cloud} for the bromide and the chloride salts [Fig. 7(b)]. We propose that if the other sulfate salts were more soluble, then T_{cloud} for MgSO_4 and K_2SO_4 would also increase dramatically at high ionic strengths. The data for MgSO_4 [Fig. 7(c)] hint that this is the case.

Examining all of the cloud-point data in Figs. 6 and 7, we note that an ionic strength of 1M, which corresponds to a Debye screening length of 3 Å, seems to be an important ionic strength in this system. For the chloride and bromide salts, T_{cloud} tends to be maximum around 1M for many of the salts tested. For $(\text{NH}_4)_2\text{SO}_4$, T_{cloud} increases sharply at about 1M.

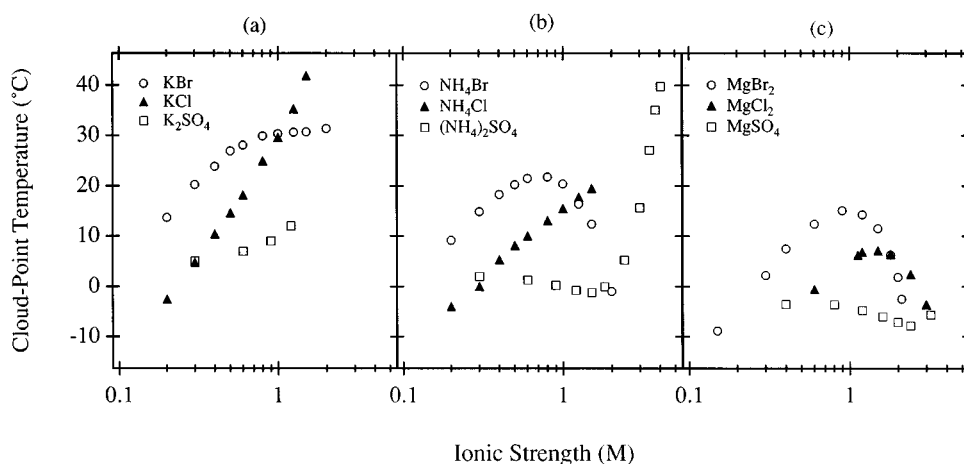


FIG. 7. Replot of a portion of the data from Fig. 6 to highlight the effect of anion identity on cloud-point temperature.

Additional experiments

As previously stated, the above data are for 20 mM HEPES, pH 7.8. This buffer is widely used by biochemists because its dissociation constant depends weakly on temperature, and it does not bind salt ions of biological importance [46]. We used a low buffer concentration so that the ionic strength of the solution was essentially due to the added salt. For the sake of completeness, we explored how T_{cloud} varies with (1) buffer identity, (2) HEPES concentration, and (3) pH . The concentration of lysozyme for these control studies was 87 mg/ml.

(1) We examined the effect of the following buffers on T_{cloud} : sodium phosphate, MOPS (3-[*N*-Morpholino]propanesulfonic acid), PIPES (Piperazine-*N,N'*-bis[2-ethanesulfonic acid]) and MES (2-[*N*-Morpholino]ethanesulfonic acid). The buffer concentration was fixed at 20 mM, $pH = 7.8$, and a range of NaCl concentration was investigated. Changing the identity of the buffer essentially shifts the cloud-point curve in Fig. 3 up or down by 1 or 2 °C, but the general shape of the curve is unchanged. We therefore conclude that our results are not critically dependent on buffer identity.

(2) We increased the concentration of HEPES buffer from 14 to 100 mM while holding the NaCl concentration at 0.4M. Increasing the buffer concentration causes T_{cloud} to decrease approximately linearly with a slope of $\Delta T_{cloud} / \Delta [HEPES] = -0.08$ °C/mM. Thus, an uncertainty of a few mM in the concentration of the buffer has a negligible effect on T_{cloud} . (It is interesting to note that increasing the HEPES concentration causes T_{cloud} to decrease. For most of the salts in Fig. 6, T_{cloud} increases with increasing ionic strength for concentrations below 1M.)

(3) We varied the pH of the sample from 7 to 8 using 20 mM HEPES for a range of NaCl concentration. Increasing the pH from 7 to 8 causes T_{cloud} to increase by about 3 °C in accord with the results of Taratuta *et al.* [13]. This implies that an uncertainty in pH of 0.4 results in an uncertainty in T_{cloud} of 1.2 °C.

DISCUSSION

We have performed a systematic investigation of liquid-liquid and solid-liquid phase separation of aqueous lysozyme solutions to explore the role of salt ions in protein interac-

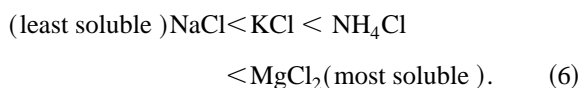
tions. We find that the cloud-point temperature depends on both the ionic strength and the identity of the added salt. The effects of cations and anions on T_{cloud} can be ranked, and this provides a rigorous test for models of protein interactions.

For a wide range of solution conditions, we find that the liquid-liquid phase boundary is below the solid-liquid phase boundary, which implies that liquid-liquid phase separation takes place in a metastable solution. This appears to be a general characteristic of concentrated protein solutions [32]. The Baxter adhesive hard sphere model predicts this type of metastability. As Ilett *et al.* [47] point out, the gas-liquid coexistence curve (which corresponds to the liquid-liquid boundary in our system) can be buried inside the fluid-crystal coexistence region in the adhesive hard sphere model. The Baxter model also accounts for the static structure factor observed in aqueous solutions of bovine γ_{II} -crystalline [35].

Comparison with other experimental results

The results of Taratuta *et al.* [13] suggest that the identity and concentration of the anion is the main factor that determines the magnitude of T_{cloud} . For the salts used in their study, NaCl, KCl, NaBr, and KBr, and for ionic strengths below 1M, our results support their claim (see Fig. 6): the curves of T_{cloud} versus ionic strength for NaCl and KCl are very similar, as are the curves for NaBr and KBr. For cations other than Na^+ and K^+ , however, we find that the identity of the cation can substantially affect the magnitude of T_{cloud} , particularly for divalent cations such as Mg^{2+} and Ca^{2+} . Thus, in general, the identity of both the anion and the cation play a role in protein interactions.

The effect of ions and pH on the solubility of lysozyme has been the subject of several studies [39–43]. Riés-Kautt and Ducruix [42] measured the solubility of lysozyme as a function of added salts at pH 4.5, $T = 18$ °C. For a series of chloride salts, they find that the protein solubility increases in the order



This ranking is fairly consistent with the cation ranking we

find based on T_{cloud} , Eq. (4), recalling that a high T_{cloud} corresponds to a low solubility (Fig. 4).

At odds with our cloud-point measurements is the fact that the solubility of lysozyme reported by Riés-Kautt and Ducruix does not increase when the ionic strength of MgCl_2 is above $1M$, as the decrease of T_{cloud} suggests it should [Fig. 6(a)]. Another discrepancy between our studies is that they were unable to grow crystals using $(\text{NH}_4)_2\text{SO}_4$. The high T_{cloud} in Fig. 6(c) for $(\text{NH}_4)_2\text{SO}_4$ indicates that the solubility of lysozyme should be low for this salt. These discrepancies may be due to the difference in pH between their study (pH 4.5) and ours (pH 7.8). At pH 4.5, lysozyme has a charge of $+11e$; at pH 7.8, its charge is $+8e$ [15].

Specific-ion effects also arise in connection with the conformational stability of proteins [48,49], the aggregation of colloidal suspensions [50], and many other physical and chemical phenomena. The effect of cations and anions on a particular system can often be ranked according to a Hofmeister series [51] that is similar to the ion rankings we find for T_{cloud} , Eqs. (4) and (5). A microscopic mechanism that fully accounts for the ubiquitous Hofmeister series remains a challenge [52].

Modeling protein interactions

The phase transitions we observe are driven by a net attraction between the protein molecules. Thus, the magnitude of T_{cloud} and T_{xtal} indicates the strength of the attraction: the stronger the attraction, the higher the transition temperatures. In this discussion, we employ ideas from colloid science to interpret our results. For other approaches to the problem of protein interactions, see Refs. [48,53,54].

The three-dimensional structure of lysozyme is very stable [15], and so it is reasonable to treat it as a rigid object. In this respect, a globular protein is more like a colloid than a polymer, which has conformational degrees of freedom. As a first approximation, therefore, we model the interaction energy between two protein molecules using the Derjaguin-Landau-Verwey-Overbeek (DLVO) theory for charged colloidal spheres [5]. Although this continuum model neglects many physical effects, it provides a valuable starting point for our discussion.

For lysozyme, the mean radius of the protein is roughly $a = 17 \text{ \AA}$ [37], and its net charge is $Q = +8e$ at pH 7.8 [15]. The total energy E in DLVO theory is the sum of the van der Waals attraction E_A and the electrostatic repulsion E_R . Let s be the distance between the surfaces of two protein molecules, and let $x = s/a$ be the dimensionless distance. For two spheres, the attractive energy is [50,55]

$$E_A = \frac{-A_H}{12} \left[\frac{4}{(x+2)^2} + \frac{4}{x^2+4x} + 2 \ln \left(\frac{x^2+4x}{(x+2)^2} \right) \right], \quad (7a)$$

where A_H is the Hamaker constant. For small x , $E_A \approx -A_H/12x$. For lysozyme in water at room temperature, Eberstein, Georgalis, and Wolfram [56] find that A_H is 7.7 kT based on dynamic light scattering measurements. Aqueous solutions of α -chymotrypsin [57] and bovine serum albumin [58] also have Hamaker constants of about 10 kT, but we note that for α -crystallin [59] A_H is 0.06 kT.

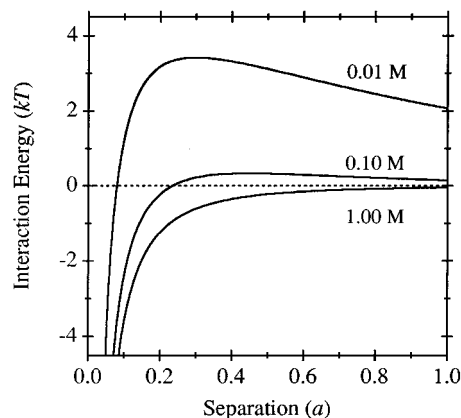


FIG. 8. Total interaction energy $E = E_R + E_A$ between two lysozyme molecules using DLVO theory, Eqs. (7), for three ionic strengths. The protein has a charge $+8e$ and a radius of $a = 17 \text{ \AA}$; the Hamaker constant is 7.7 kT.

Since Q is independent of ionic strength near pH 7.8 [15], we use the constant-charge model for the repulsive energy [5,60]:

$$E_R = \frac{Q^2 e^{-\kappa a x}}{4 \pi \epsilon \epsilon_0 a (x+2) (1 + \kappa a)^2}, \quad (7b)$$

where κ^{-1} is the Debye screening length, ϵ is the dielectric constant of the solution and ϵ_0 is the permittivity of free space. At 25°C the Debye length of aqueous solutions is $\kappa^{-1} = 3 \text{ \AA} / \sqrt{I}$, where I is the ionic strength of the solution in moles/l. The essential point is that E_R decays exponentially with κs .

In Fig. 8, we plot the total interaction energy $E = E_R + E_A$ for three ionic strengths. As expected, increasing the ionic strength of the solution decreases the repulsive barrier. Note that for ionic strengths above $0.1M$, which corresponds to our experimental situation, the barrier is less than 1 kT. For such a weak repulsion, the protein molecules would aggregate instantaneously, as the following calculation shows.

The time scale for aggregation is $t_{\text{agg}} = 3 \eta W / 4 k T N$, where η is the solvent viscosity, N is the number of protein molecules per unit volume, and $W = 2 \int_0^\infty e^{E/kT} (x+2)^{-2} dx$ is the stability ratio [61,62]. For a lysozyme concentration of 87 mg/ml, $N = 3.8 \times 10^{18}/\text{ml}$ and $t_{\text{agg}} = (4.6 \times 10^{-8} \text{ s}) W$. We numerically integrated the curves in Fig. 8 to obtain W at each ionic strength: $W(0.01M) = 6.9$, $W(0.1M) = 1.0$, $W(1.0M) = 0.85$. Thus, even for $0.01M$ ionic strength, DLVO theory predicts that the protein aggregates in $3 \times 10^{-7} \text{ s}$. This does not occur in our experiments. Solutions with an ionic strength of $0.01M$ are stable for months, and they do not crystallize or precipitate. Decreasing the value of the Hamaker constant to 1 kT does not significantly increase the stability factor. Clearly there must be some other repulsive interaction that prevents the protein from aggregating rapidly; electrostatic repulsion is not enough.

Victor and Hansen [63] predict that liquid-liquid phase separation can arise from the secondary minimum of the DLVO potential. For our experimental system the secondary

minimum is negligible. To achieve a secondary minimum of depth $\sim kT$, the protein would have to be 10^3 times bigger than it actually is. This raises an interesting possibility. Dynamic light scattering studies [24,56,64] show that lysozyme forms aggregates when the solution is supersaturated ($T < T_{\text{xtal}}$). The interaction energy between micrometer-sized aggregates could have a secondary minimum of sufficient depth to drive liquid-liquid phase separation. This might explain why liquid-liquid phase separation occurs in supersaturated solutions; that is, it might explain why $T_{\text{cloud}} < T_{\text{xtal}}$.

Hydration force

Our analysis of DLVO theory shows that the electrostatic repulsion is not strong enough to prevent the protein from instantaneously aggregating at the high ionic strengths used in our experiments. We believe that the repulsive hydration force [5,65] is what prevents lysozyme from aggregating. It is well established that water molecules strongly bind to protein surfaces [66]. The hydration force reflects the work required to remove this bound water when two protein molecules approach each other. Osmotic-stress measurements by Leikin, Rau, and Parsegian [67,68] demonstrate the importance of hydration forces between collagen triple helices. Dym, Mevarech, and Sussman [69] hypothesize that hydration forces prevent halophilic proteins from aggregating at high salt concentrations.

Pashley [70–73] and Pashley and Israelachvili [74] have measured the hydration force between molecularly smooth mica surfaces in salt solutions. For salt concentrations above $10^{-3}M$, they find that the repulsion depends on the identity of the cation: the more hydrated the cation, the greater the repulsion. When cations bind to the negative charged mica surfaces, they presumably retain some of their waters of hydration. The highly hydrated ions, such as Mg^{2+} and Ca^{2+} , result in the greatest repulsion because they carry the most water with them.

It is important to keep in mind that the charge on a protein is due to discrete positively and negatively charged surface groups. In lysozyme, the average distance between these charges is about 10 \AA [37]. For ionic strengths above $0.1M$, the Debye screening length is smaller than this distance, and the surface charges are essentially screened from one another. This explains why both positive and negative ions can bind to lysozyme even though the net charge of the protein is positive at $pH 7.8$.

We are thus lead to consider the protein interaction to be the sum of van der Waals attraction and repulsion due to hydration. Israelachvili [5] has tabulated the hydrated radii of various ions. For cations, the hydrated radii increase in the following order:

$$\text{(smallest) } K^+ < Na^+ < Li^+ < Ca^{2+} < Mg^{2+} \text{ (biggest).} \quad (8)$$

This order correlates very nearly with the order we find for the cloud-point temperatures, Eq. (4). The smaller the bound ion is, the closer the protein surfaces are able to approach each other; the closer they approach, the greater the van der Waals attraction and the higher the cloud-point temperature. Furthermore, since the number of cations bound to a protein

increases with salt concentration [75], we expect the influence of cations on T_{cloud} to increase with ionic strength. This agrees with Fig. 6: at low ionic strength, T_{cloud} is slightly dependent on cation identity, whereas at high ionic strength, T_{cloud} is highly cation specific.

The situation for the anions is less clear. The radius of hydration for Br^- and Cl^- are equal [5], suggesting that the hydration force is not strongly dependent on anion identity. We propose that the anion identity affects T_{cloud} by changing the magnitude of the Hamaker constant. Lifshitz theory [5] shows that A_H depends on the index of refraction of the medium in which the protein is dissolved. Using tabulated data [76], we find that the index of refraction increases approximately linearly with increasing ionic strength over the range 0 to $5M$ for the salts used in our study. The slope of this increase depends strongly on anion identity and is weakly dependent on cation identity. This suggests that anion identity plays a more important role than cation identity in setting the magnitude of the Hamaker constant. A rigorous determination of A_H is needed to test this hypothesis.

Solid-liquid transition

An essential distinction between liquid-liquid and solid-liquid phase separation is the nature of the protein-rich phase. In liquid-liquid phase separation the dense phase is simply a concentrated protein solution. In solid-liquid phase separation the dense phase is a crystal, and the proteins form intermolecular bonds at specific sites. We thus expect the attraction between the proteins to be stronger in a crystal than in a protein-rich liquid phase, and as a consequence, we expect $T_{\text{cloud}} < T_{\text{xtal}}$, which is what occurs experimentally.

The next issue is to understand why it takes hours or days for supersaturated protein solutions to crystallize. Solutions of lysozyme and calf lens proteins [32] can be cooled $30\text{--}40^\circ\text{C}$ below T_{xtal} and do not form macroscopic crystals. Kinetic arguments do not seem to be the answer, since the rotational diffusion coefficient for lysozyme is quite large $3 \times 10^7 \text{ s}^{-1}$, [75] indicating that the proteins should be able to align quickly and form a crystal. Pusey [43] claims that there may be an activation barrier associated with the formation of intermolecular contacts due to the breaking of protein-solvent interactions in favor of protein-protein interactions. Evidence for the removal of parts of the hydration shell comes from the release of Cl^- , observed using stopped-flow fluorescence quenching [43].

SUMMARY

The study of phase transitions in concentrated protein solutions provides one with a simple means of assessing the effect of solution conditions on the strength of protein interactions. The data presented in this paper demonstrate that the effect of salt on protein interactions depends sensitively on the identities of the cation and anion in solution. We find that DLVO theory cannot account for our observations and that hydration forces play an important role in protein interactions.

In continuing studies, we will explore the effects of changing the protein charge (pH) and of adding polyethylene glycol, a nonionic polymer, to the solution. Much more theoretical work is needed to fully interpret our experimental results. A deeper understanding of how solution conditions affect protein interactions is a first step in addressing important problems in biology, chemistry, and medicine.

ACKNOWLEDGMENTS

We are grateful to Steve Vierck, Aaron Nelson, Adam Johnston, Steve Schiveley, and Steve Attinasi for their many contributions to this project. We thank John Perona for illuminating discussions about protein crystals. This research was supported by a Bristol-Myers Squibb Company Award of Research Corporation and the Murdock Charitable Trust.

-
- [1] D.S. Goodsell, *Trends Biochem. Sci.* **16**, 203 (1991).
- [2] A. B. Fulton, *Cell* **30**, 345 (1982).
- [3] D. S. Goodsell, *The Machinery of Life* (Springer-Verlag, New York, 1993).
- [4] G. J. Wistow and J. Piatigorsky, *Annu. Rev. Biochem.* **57**, 479 (1988).
- [5] J. Israelachvili, *Intermolecular and Surface Forces*, 2nd ed. (Academic, San Diego, 1992).
- [6] D. F. Evans and H. Wennerström, *The Colloidal Domain: Where Physics, Chemistry, Biology, and Technology Meet* (VCH Publishers, New York, 1994).
- [7] H. G. Bungenberg de Jong, in *Colloid Science, Vol. II*, edited by H. R. Kruyt (Elsevier, Amsterdam, 1949), p. 232.
- [8] J. S. Rowlinson and F. L. Swinton, *Liquids and Liquid Mixtures*, 3rd ed. (Butterworth, London, 1982).
- [9] P. Flory, *Principles of Polymer Chemistry* (Cornell University Press, Ithaca, 1971).
- [10] *Michelle's, Membranes, Microemulsions, and Monolayers*, edited by W. M. Gelbart, A. Ben-Shaul, and D. Roux (Springer-Verlag, New York, 1994).
- [11] C. Ishimoto and T. Tanaka, *Phys. Rev. Lett.* **39**, 474 (1977).
- [12] G. D. J. Phillies, *Phys. Rev. Lett.* **55**, 1341 (1985).
- [13] V. G. Taratuta, A. Holschbach, G. T. Thurston, D. Blank-schtein, and G. B. Benedek, *J. Phys. Chem.* **94**, 2140 (1990).
- [14] W. J. Fredericks, M. C. Hammonds, S. B. Howard, and F. Rosenberg, *J. Cryst. Growth* **141**, 183 (1994).
- [15] C. Tanford and R. Roxby, *Biochemistry* **11**, 2192 (1972).
- [16] A. J. Sophianopoulos, C. K. Rhodes, D. N. Holcomb, and K. E. Van Holde, *J. Biological Chem.* **237**, 1107 (1962).
- [17] *Crystallization of Nucleic Acids and Proteins*, edited by A. Ducruix and R. Giegé (Oxford University Press, New York, 1992).
- [18] T. Arakawa and S. N. Timasheff, *Methods Enzym.* **114**, 49 (1985).
- [19] A. McPherson, *Methods Biochem. Anal.* **23**, 249 (1976).
- [20] A. McPherson, *Methods Enzym.* **114**, 112 (1985).
- [21] F. Rosenberger, S. B. Howard, J. W. Sowers, and T. A. Nyce, *J. Cryst. Growth* **129**, 1 (1993).
- [22] A. V. Elgersma, M. Ataka, and T. Katsura, *J. Cryst. Growth* **122**, 31 (1992).
- [23] M. Ataka and M. Asai, *Biophys. J.* **58**, 807 (1990).
- [24] Z. Kam, H. B. Shore, and G. Feher, *J. Mol. Biol.* **123**, 539 (1978).
- [25] While the onset and detection of liquid-liquid phase separation is rapid, it takes days for the sample to equilibrate and separate into two clear liquid phases separated by a sharp meniscus. Centrifugation can be used to accelerate the separation process, as discussed in Ref. [13].
- [26] R. J. Siezen, M. R. Fisch, C. Slingsby, and G. B. Benedek, *Proc. Natl. Acad. Sci. USA* **82**, 1701 (1985).
- [27] J. I. Clark and D. Carper, *Proc. Natl. Acad. Sci. USA* **84**, 122 (1987).
- [28] C. T. Noguchi and A. N. Schechter, *Annu. Rev. Biophys. Biophys. Chem.* **14**, 239 (1985).
- [29] C. R. Middaugh, B. Gerber-Jensen, A. Harvitz, A. Paluszek, C. Scheffel, and G. W. Litman, *Proc. Natl. Acad. Sci. USA* **75**, 3440 (1978).
- [30] J. A. Thomson, P. Schurenberger, G. M. Thurston, and G. B. Benedek, *Proc. Natl. Acad. Sci. USA* **84**, 7079 (1987).
- [31] M. L. Broide, C. R. Berland, J. Pande, O. Ogun, and G. B. Benedek, *Proc. Natl. Acad. Sci. USA* **88**, 5660 (1991).
- [32] C. R. Berland, G. M. Thurston, M. Kondo, M. L. Broide, J. Pande, O. Ogun, and G. B. Benedek, *Proc. Natl. Acad. Sci. USA* **89**, 1214 (1992).
- [33] P. Schurtenberger, R. A. Chamberlin, G. M. Thurston, J. A. Thomson, and G. B. Benedek, *Phys. Rev. Lett.* **63**, 2064 (1989).
- [34] B. M. Fine, J. Pande, A. Lomakin, O. O. Ogun, and G. B. Benedek, *Phys. Rev. Lett.* **74**, 198 (1995).
- [35] B. M. Fine, A. Lomakin, O. O. Ogun, and G. B. Benedek, *J. Chem. Phys.* **104**, 326 (1996).
- [36] P. L. San Biagio and M. U. Palma, *Biophys. J.* **60**, 508 (1991).
- [37] D. Voet and J. Voet, *Biochemistry* (Wiley, New York, 1990).
- [38] *EDTA, B: Determination of Cadmium, Calcium, Magnesium, and Manganese(II) by Complex Formation with EDTA* (Aldrich Chemical, Milwaukee, 1990).
- [39] E. Cacioppo and M. L. Pusey, *J. Cryst. Growth* **114**, 286 (1991).
- [40] F. Ewing, E. Forsythe, and M. Pusey, *Acta Crystallogr. D* **50**, 424 (1994).
- [41] J. P. Guilloateau, M. M. Riés-Kautt, and A. F. Ducruix, *J. Cryst. Growth* **122**, 223 (1992).
- [42] M. M. Riés-Kautt and A. F. Ducruix, *J. Bio. Chem.* **264**, 745 (1989).
- [43] M. L. Pusey, *J. Cryst. Growth* **122**, 1 (1992).
- [44] S. D. Durbin and G. Feher, *J. Cryst. Growth* **76**, 583 (1986).
- [45] G. L. Gilliland, *J. Cryst. Growth* **90**, 51 (1988).
- [46] N. E. Good, G. D. Winget, W. Winter, T. N. Connolly, K. Iazna, and R. M. M. Singh, *Biochem.* **5**, 467 (1966).
- [47] S. M. Ilett, A. Orrock, W. C. K. Poon, and P. N. Pusey, *Phys. Rev. E* **51**, 1344 (1995).
- [48] T. Arakawa and S. N. Timasheff, *Biochem.* **21**, 6545 (1982).
- [49] P. H. von Hippel and A. Hamabata, *J. Mechanochem. Cell Motility*, **2**, 127 (1973).
- [50] P. C. Hiemenz, *Principles of Colloid and Surface Chemistry*, 2nd ed. (Marcel Dekker, New York, 1986).

- [51] K. D. Collins and M. W. Washabaugh, *Q. Rev. Biophys.* **18**, 323 (1985).
- [52] V. A. Parsegian, *Nature* **378**, 335 (1995).
- [53] L. J. D. Frink and F. van Swol, *J. Chem. Phys.* **100**, 9106 (1994).
- [54] C. Liu, A. Lomakin, G. M. Thurston, D. Hayden, A. Pande, J. Pande, O. Ogun, N. Asherie, and G. B. Benedek, *J. Phys. Chem.* **99**, 454 (1995).
- [55] W. B. Russel, D. A. Saville, and W. R. Schowalter, *Colloidal Dispersions* (Cambridge University Press, Cambridge, 1989).
- [56] W. Eberstein, Y. Georgalis, and S. Wolfram, *J. Cryst. Growth* **143**, 71 (1994).
- [57] C. A. Haynes, K. Tamura, H. R. Körfer, H. W. Blanch, and J. M. Prausnitz, *J. Phys. Chem.* **96**, 905 (1992).
- [58] S. N. Srivastava, *Z. Phys. Chem.* **233**, 237 (1966).
- [59] J. -Z. Xia, T. Aerts, K. Donceel, and J. Clauwaert, *Biophys. J.* **66**, 861 (1994).
- [60] J. C. Crocker and D. G. Grier, *Phys. Rev. Lett.* **73**, 352 (1994).
- [61] M. L. Broide and R. J. Cohen, *J. Colloid Interface Sci.* **153**, 493 (1992).
- [62] D. H. Everett, *Basic Principles of Colloid Science* (Royal Society of Chemistry, London, 1988).
- [63] J. M. Victor and J. P. Hansen, *J. Chem. Soc., Faraday Trans. 2* **81**, 43 (1985).
- [64] M. Skouri, J. P. Munch, B. Lorber, R. Giegé, and S. Candau, *J. Cryst. Growth* **122**, 14 (1992).
- [65] S. Leiken, V. A. Parsegian, D. C. Rau, and R. P. Rand, *Annu. Rev. Phys. Chem.* **44**, 369 (1993).
- [66] J. T. Edsall and H. A. McKenzie, *Adv. Biophys.* **16**, 53 (1983).
- [67] S. Leikin, D. C. Rau, and V. A. Parsegian, *Proc. Natl. Acad. Sci. USA* **91**, 276 (1994).
- [68] S. Leikin, D. C. Rau, and V. A. Parsegian, *Nature Struct. Biol.* **2**, 205 (1995).
- [69] O. Dyn, M. Mevarech, and J. L. Sussman, *Science* **267**, 1344 (1995).
- [70] R. M. Pashley, *J. Colloid Interface Sci.* **83**, 531 (1981).
- [71] R. M. Pashley, *J. Colloid Interface Sci.* **80**, 153 (1981).
- [72] R. M. Pashley, *Adv. Colloid Interface Sci.* **16**, 57 (1982).
- [73] R. M. Pashley, *Chemica Scripta* **25**, 22 (1985).
- [74] R. M. Pashley, and J. N. Israelachvili, *J. Colloid Interface Science* **97**, 446 (1984).
- [75] K. E. van Holde, *Physical Biochemistry*, 2nd ed. (Prentice-Hall, Englewood Cliffs, NJ, 1985).
- [76] *Handbook of Chemistry and Physics*, 54th ed., edited by R. C. Weast (CRC Press, Cleveland, 1973).